Associated Interests

- **Surface Reflectance Intermediate Product**
  - **Insufficient performance for EVI (-NGST, August 2003)**
  - **Collaboration with Lyapustin, Vermote and Wolfe**

- **“The Products Formerly Known As VVI2P”**
  - **LAI and FPAR**

Develop Proxy Data Transformations

"Spectral - spatial transfer functions" to optimally relate MODIS and ASTER/ETM+ characteristics to the VIIRS characteristics

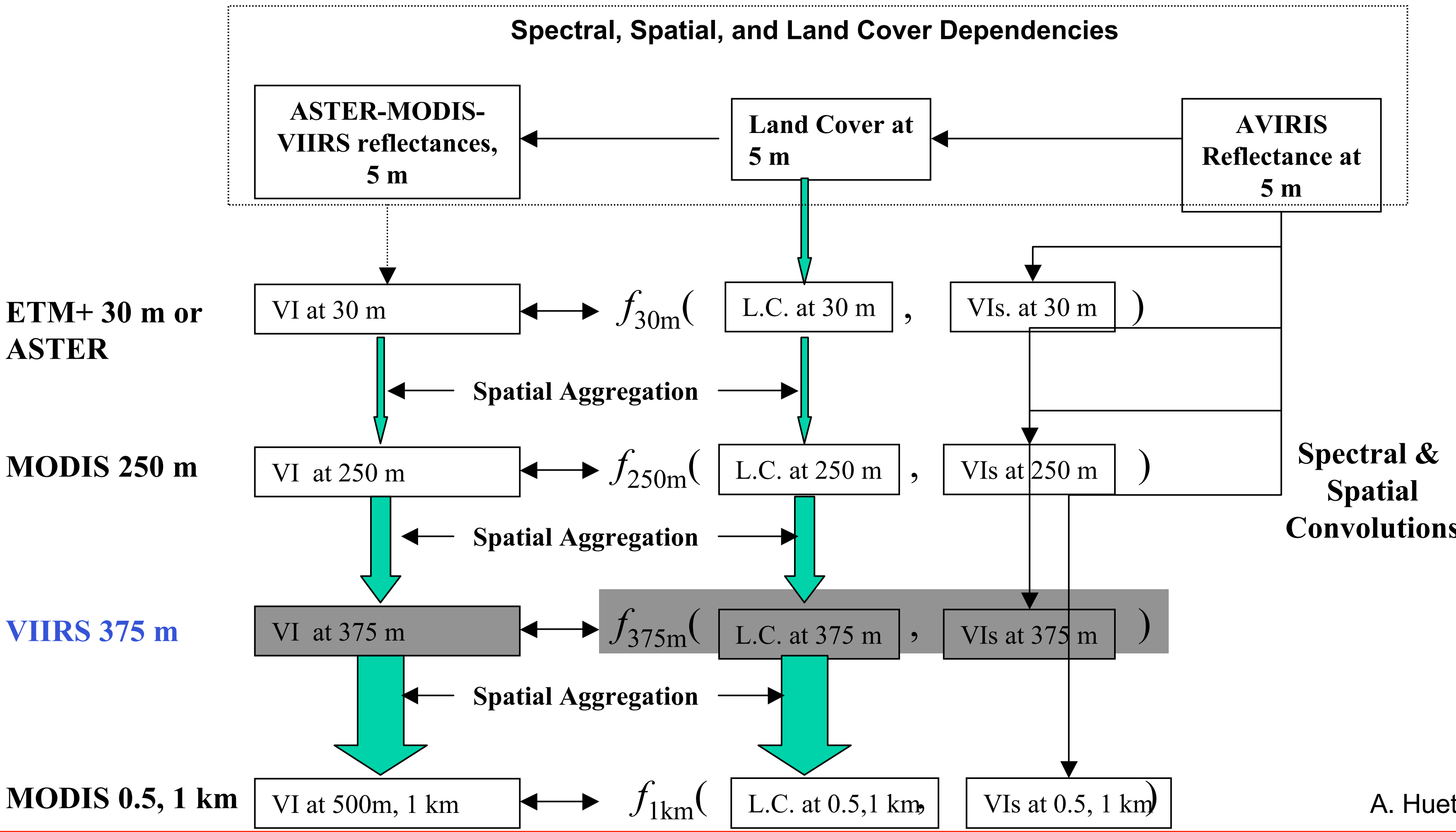

A. Huete

Entrain EDR Algorithms in MODIS Stream

- **Proxy Data Sets: VIIRS-looking data derived from MODIS L1b Data**
- **Implementation of VIIRS prototypes in MODAPS Subsetting Stream**
  - **26 * 200km x 200km Core Sites**
  - **274 * 7km x 7km ORNL ASCII Sites**

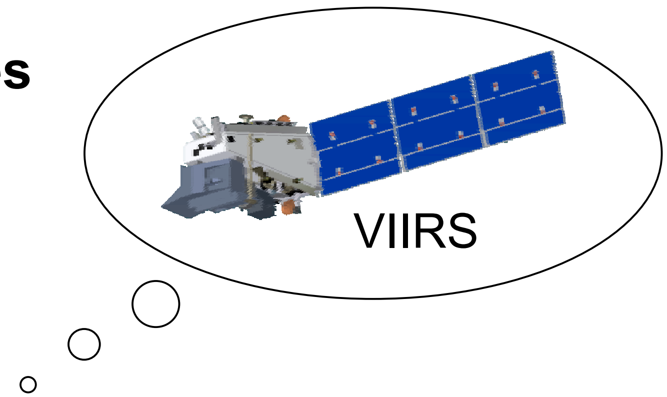

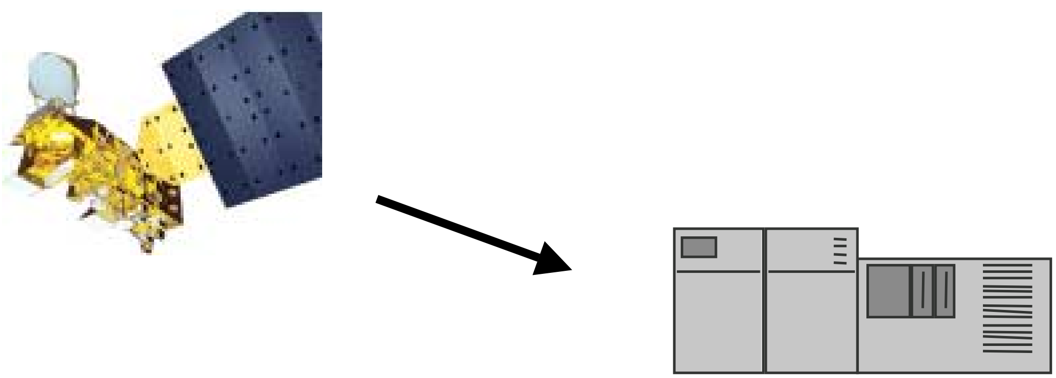

Operational Generation of EDRs from Proxy-VIIRS Data

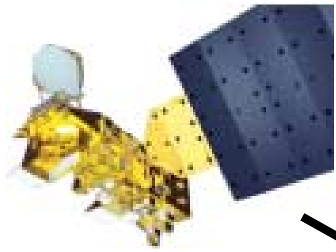

MODIS

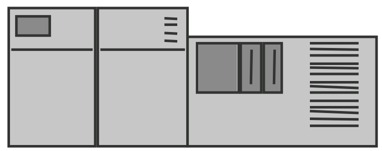

MODAPS

7 km x 7 km Subset of MODIS Tile

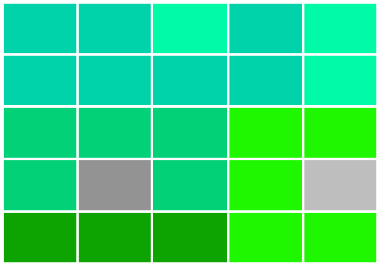

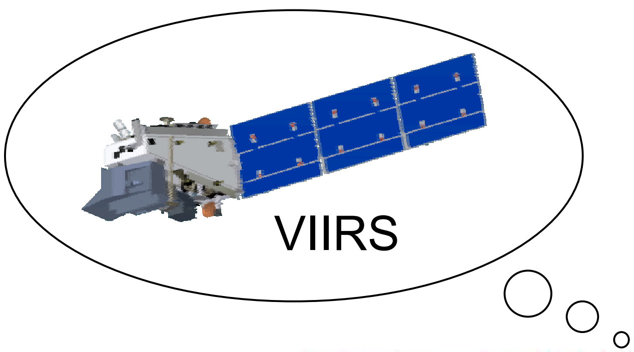

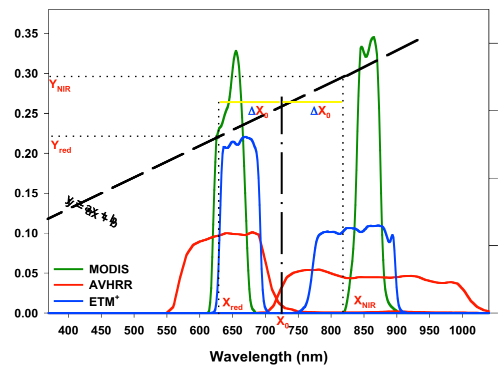

Spectral-Spatial Transformation

Assess Performance

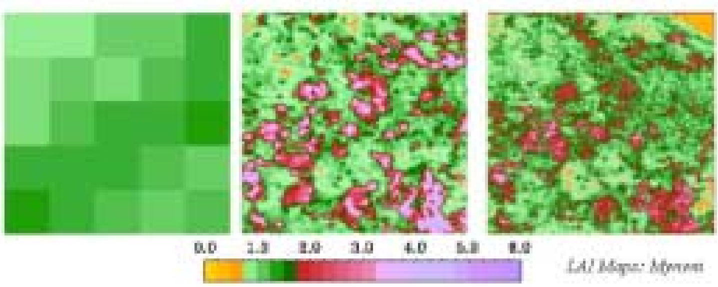

VI: Model-based Estimations of EDR Uncertainty

$$\varepsilon(\text{ EDR }) = fcn(\ \varepsilon(\text{algorithm model}),\ \varepsilon(\text{ algorithm input }))$$

Accuracy in the retrievals can not exceed the summed accuracy of the data and model

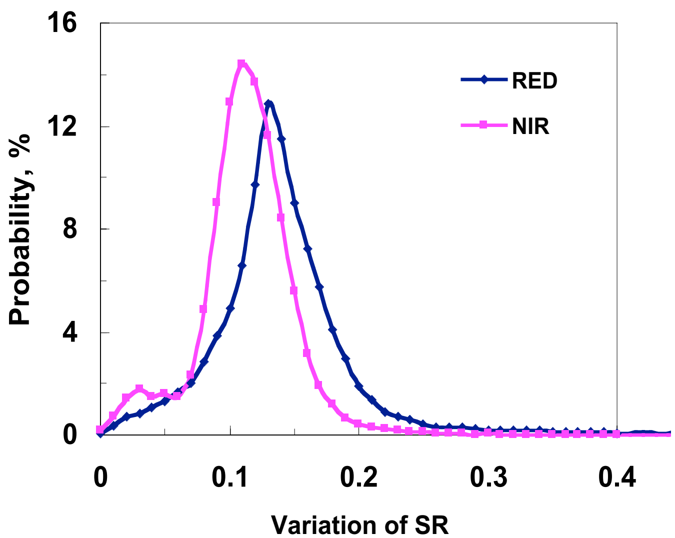

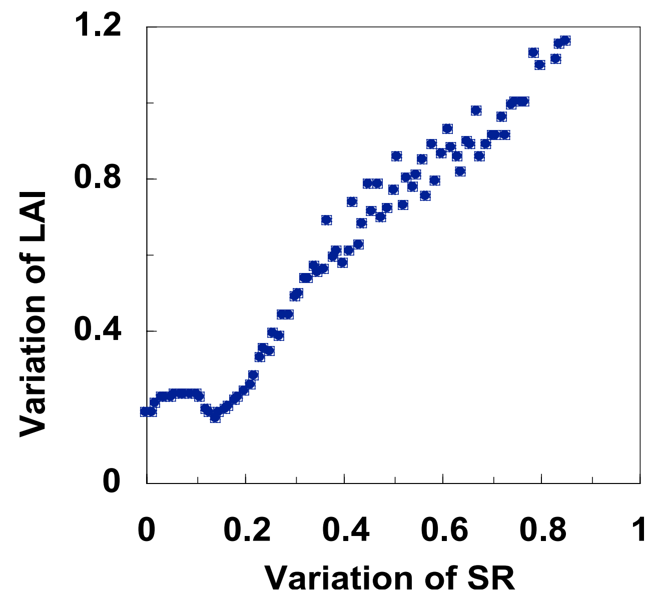

- **VIIRS Model uncertainty: zero for VI, but non-zero for albedo and LST**
- **Analysis performed following the MODIS LAI/FPAR algorithm (figures above)**

R. Myneni

VI: Deriving Further Biophysical Products (LAI, FPAR)

MODIS LAI/FPAR main algorithm ingests surface reflectances

MODIS LAI/FPAR back-up algorithm ingests NDVI

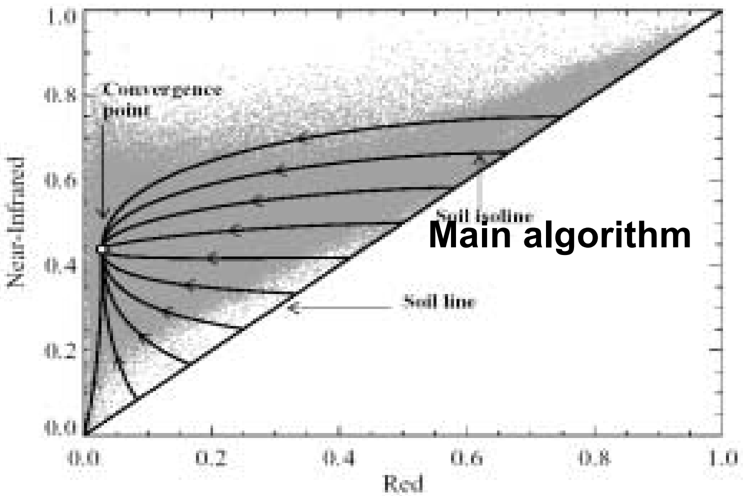

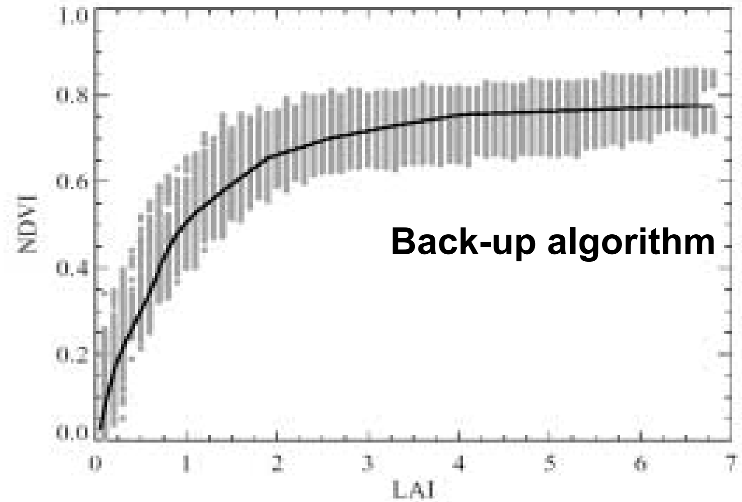

- **Adapt algorithms to ingest proxy-VIIRS surface reflectances and NDVI, respectively**
- **Characterize differences betweens the respective LAI and FPAR results**
- **VIIRS albedo also can generated internally by the main algorithm**

R. Myneni

VI: Sensitivity to Vegetation Dynamics Resulting from Climate Change

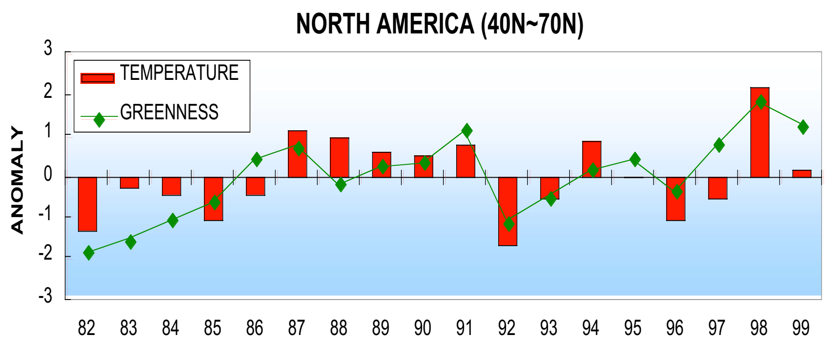

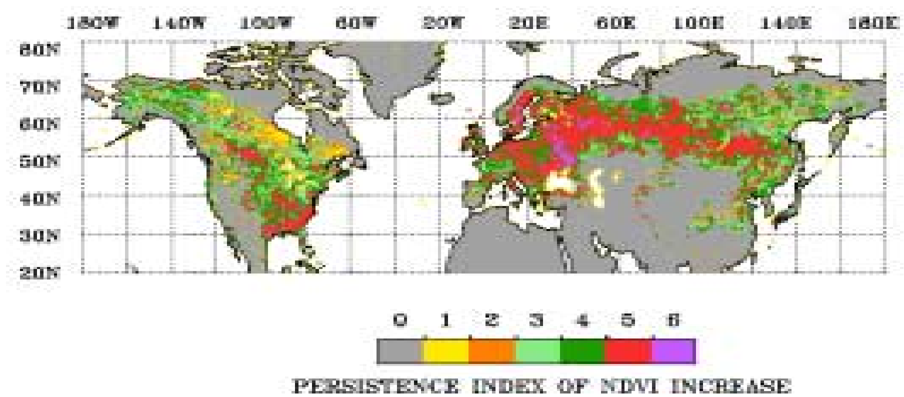

- **Identify areas significantly affected by climate change by determining the *persistence index** in an AVHRR NDVI time series (1981-2005) over northern latitudes**
- **Characterize signals of change in these areas, using MODIS data (2000-2005) as a VIIRS data proxy**
- **Estimate VIIRS VI sensitivity by evaluating the change signatures with their associated noise levels for different degrees of persistence index**

*** persistence index determines where NDVI increased consistently, as opposed to NDVI trending**

R. Myneni

Directional effects in observations of land surface temperature with AVHRR over Africa

Ana C.T. Pinheiro,
Jeffrey L. Privette, and
Compton J. Tucker

Faculdade de Ciências e Tecnologia
Universidade Nova de Lisboa

Goddard Space Flight Center
National Aeronautics and Space Administration

New AVHRR LST over Africa

- Period: lifetime of NOAA-14 (1995-2000)
- Pixel resolution: 8 km (Albers equal area projection)
- Overpass time: Day and night
- Coverage: daily
- Full swath width of the scanning

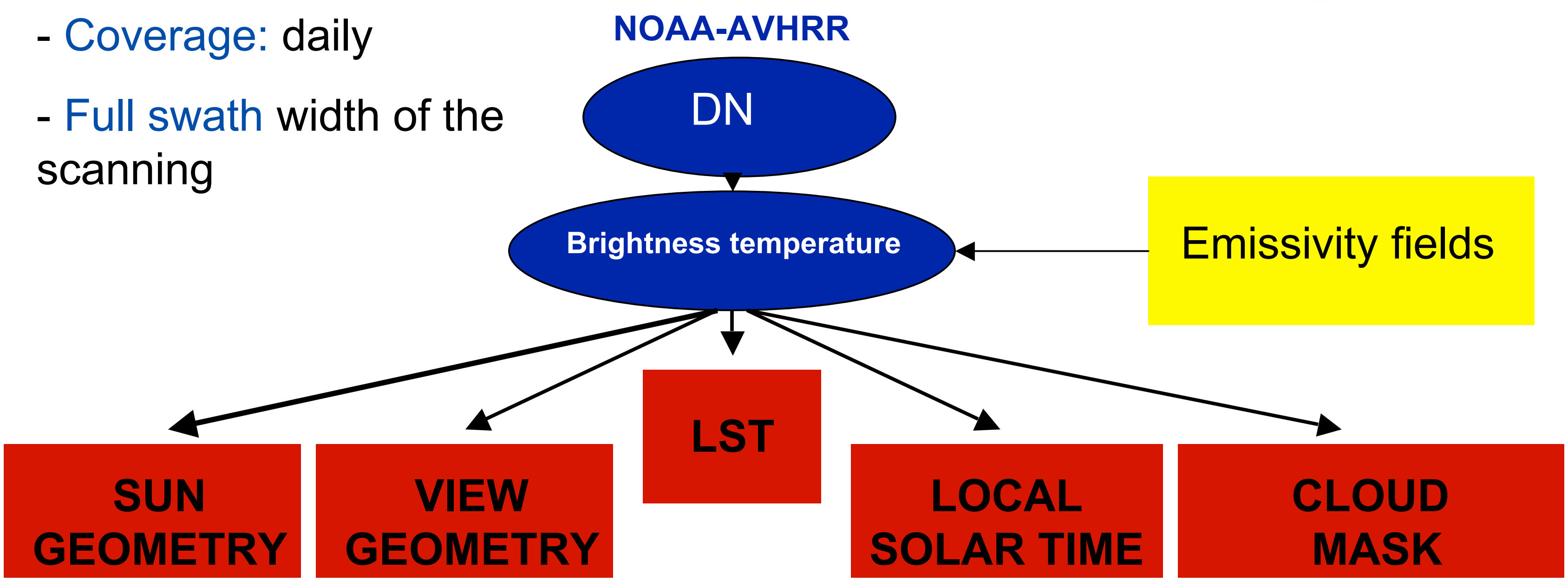

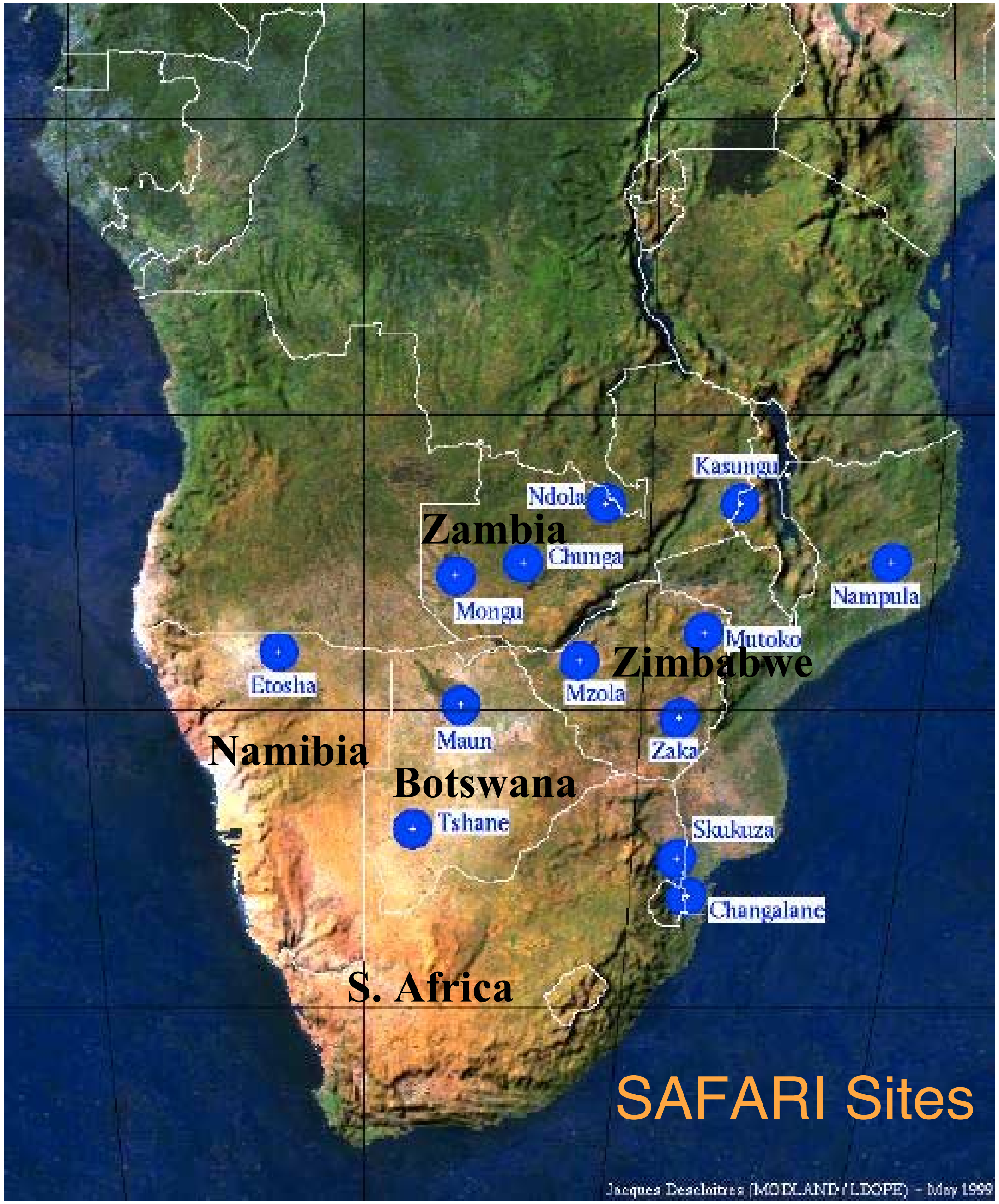

Southern Africa

13 Sites Covering Range Land/Climate Regimes

All have MODLAND products subsetted and posted at ORNL DAAC

Further Supported through MODLAND and SAFARI 2000 Validation Scene Purchases

Mongu and Skukuza were Core Sites with Towers and 3 Years of Field Data

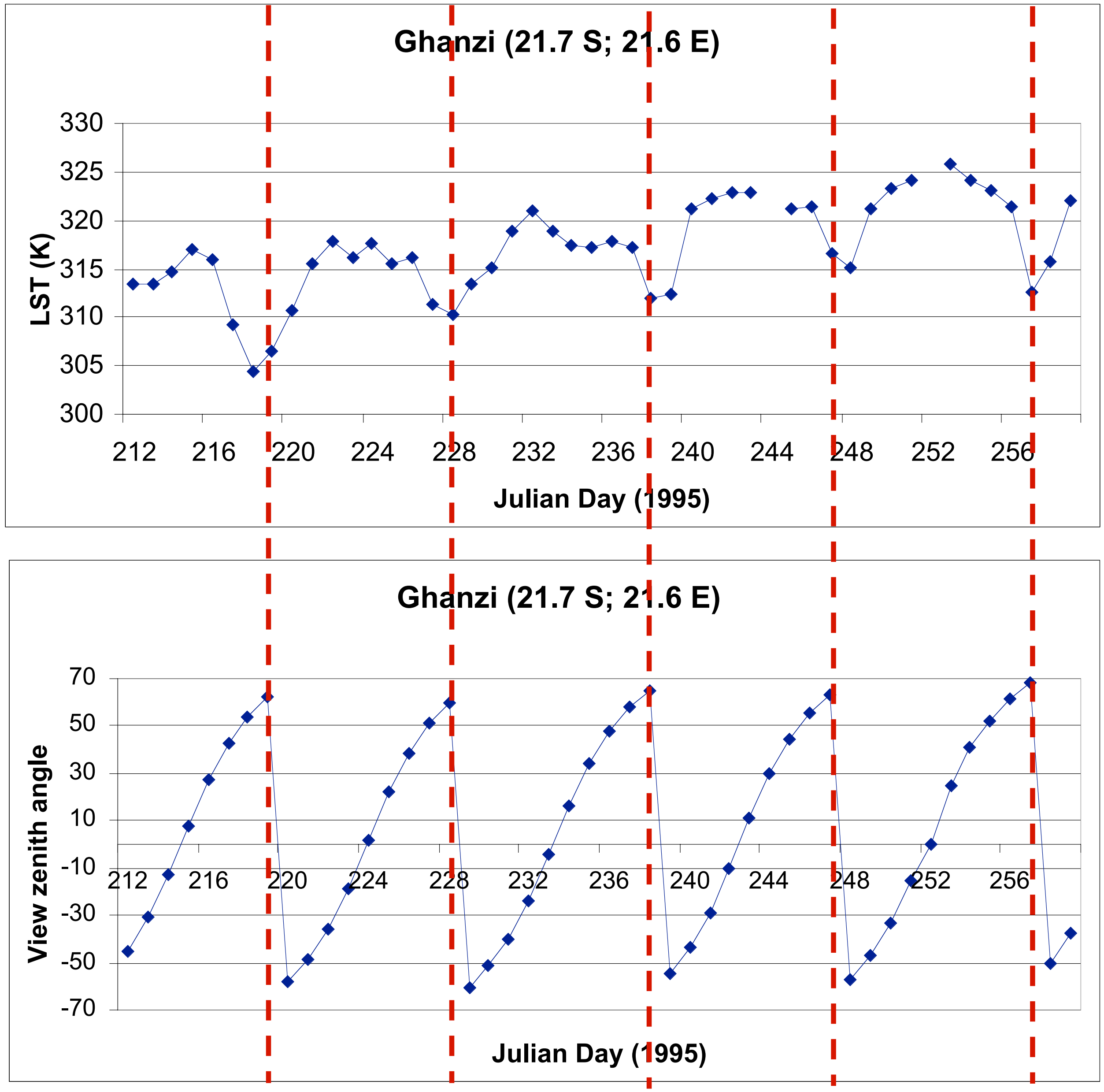

Ghanzi (21.7 S; 21.6 E)
LST (K)
330
325
320
315
310
305
300
212
216
220
224
228
232
236
240
244
248
252
256
Julian Day (1995)
Ghanzi (21.7 S; 21.6 E)
View zenith angle
70
50
30
10
-10
-30
-50
-70
212
216
220
224
228
232
236
240
244
248
252
256
Julian Day (1995)

Testing the approach at local scale: Skukuza, SA

Comparison between pyrgeometer LWUP[1] and hemispherically integrated emsemble temperature (Gaussian quadrature)

$$\langle M(h) \rangle = \frac{\sigma}{\pi} \int_{\theta=0}^{\frac{\pi}{2}} \int_{\phi=0}^{2\pi} \left(\sum_{k=1}^{N} \varepsilon_k T_{sk}{}^4 X_{(k,\theta,\phi)} \right) \partial\phi \partial\theta$$

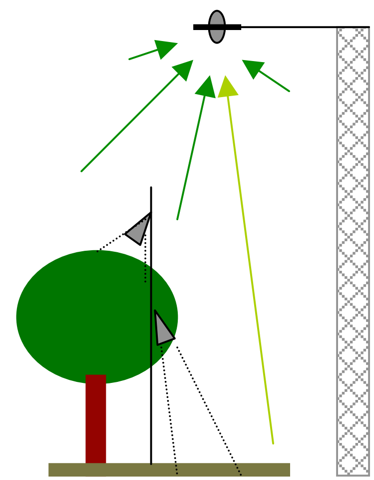

with $\chi_{k,\theta,\phi}$ generated by geometrical-optical **(GO)** component of the GORT model (Ni et al., 1999).

[1] *pyrgeometer data provided by Niall Hanan, CSU*

Orbital drift effect: time of observation

Satellite launch (1995): **~ 1:30 PM**

Satellite demise (2000): **~ 4:00 PM**

Very different temperatures of endmembers

Angular effects in AVHRR LST are minimized in the last years of satellite life due to orbital drift.

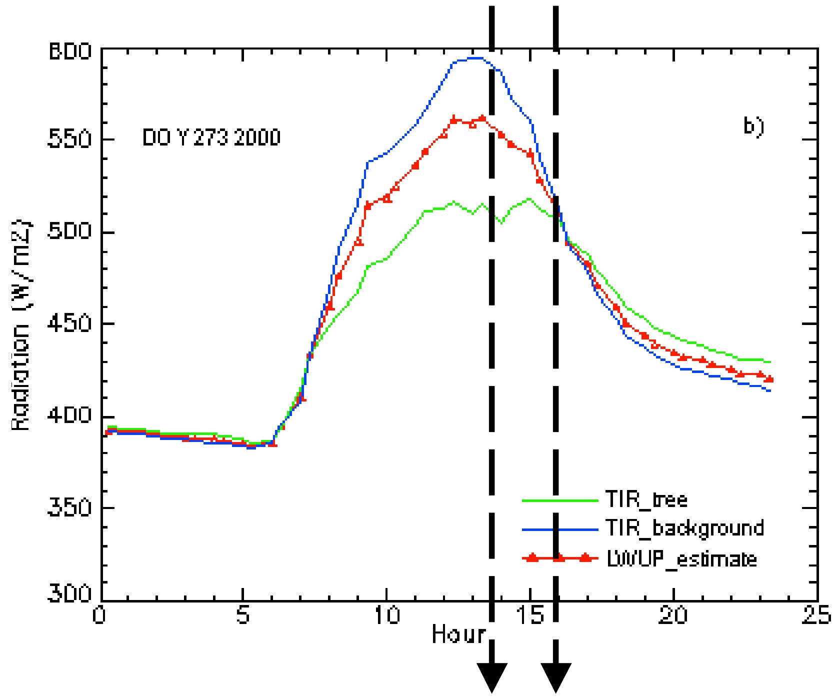

Observation time: **1:30 PM** **4:00 PM**

Effects of view-target-sun geometry variation

- **flat surfaces:** time of observation (sun geometry)
- **3-D structured surfaces:** sun and view geometry

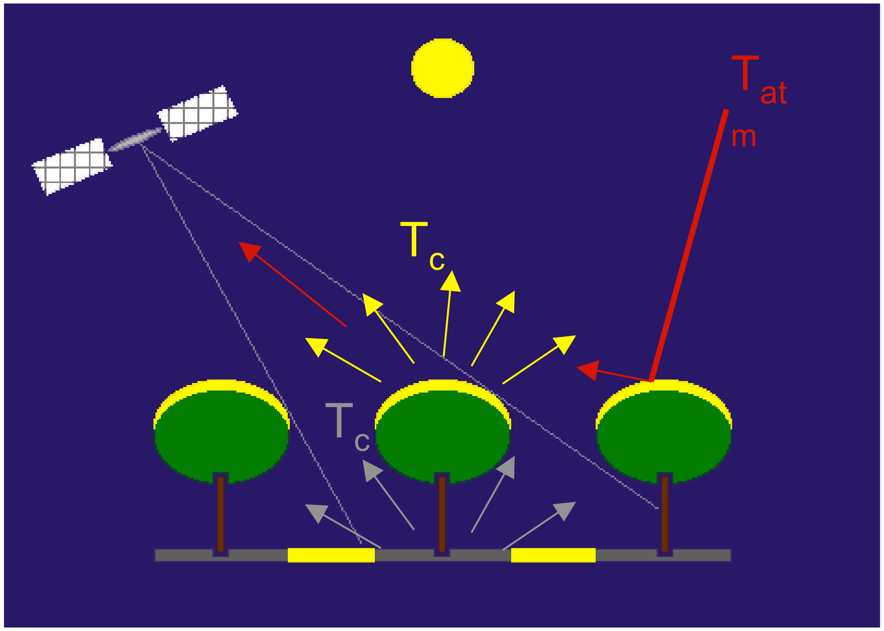

$$L(\lambda,\theta,\phi,h) = L(\lambda,\theta,\phi,0)\tau_\lambda(\phi,\theta) + \int_0^h L(\lambda,T_{at}(z))\frac{\partial\tau_\lambda(\phi,\theta,z)}{\partial z}dz$$

$$L(\lambda,\theta,\phi,0) = B(T_{rd}) = \varepsilon_\lambda B(T_s) + (1-\varepsilon_\lambda)(E_{at}/\pi)$$

Continental scale: vegetation structure

Continuous fields: woody, herbaceous and barren cover
(DeFries et al., 2000)

Land cover map
(Hansen et al., 2000)

Vegetation map of Africa
(White, 1983)

Decision tree like approach

- **Average crown vertical radius**
- **Maximum tree height**
- **Minimum tree height**
- **Average crown horizontal radius**

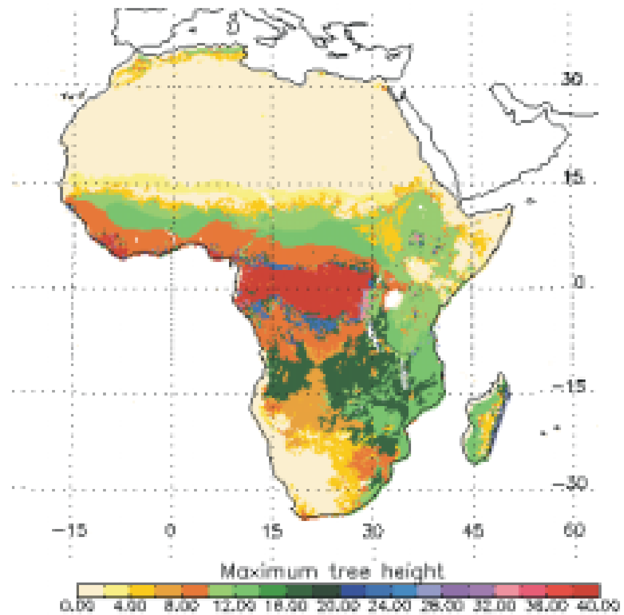

Maximum tree height

African Structure Maps

Pinheiro et al., 2004

Maximum tree height

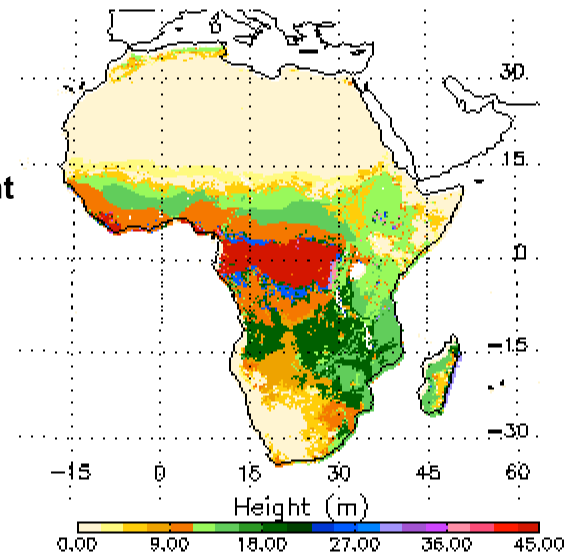

Minimum tree height

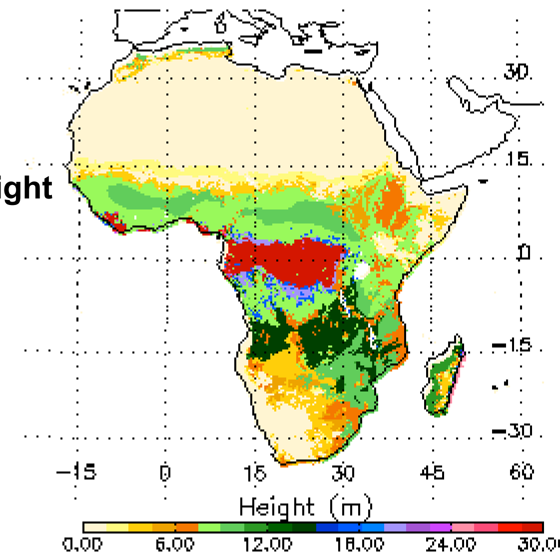

Average crown diameter

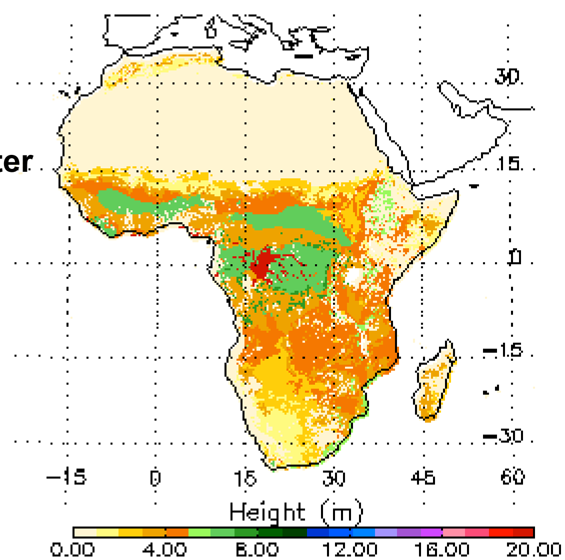

Average crown height

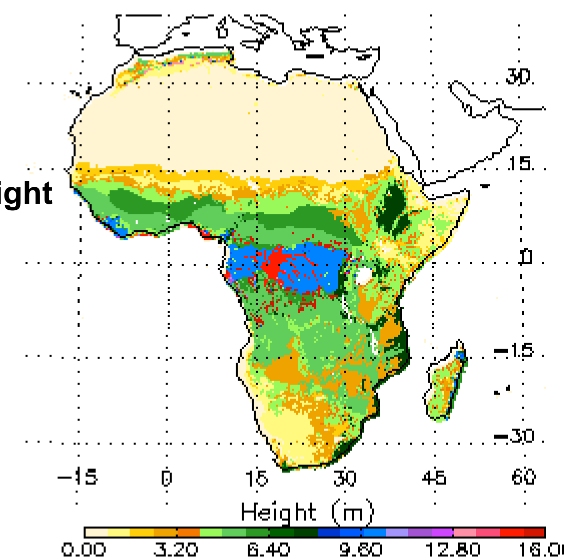

VI, Albedo & LST

Continental scale: projected fractional covers

view-target-sun geometry

AVHRR illumination geometry

AVHRR observation geometry

Structural information

Continuous fields: woody, herbaceous and barren cover

Average crown vertical radius

Maximum tree height

Minimum tree height

Average crown horizontal radius

Geometric-optical model

4 projected endmember fractions

(sunlit and shaded crown, sunlit and shaded background)

Continental scale: projected fractions

Sunlit crown projected fractions for two days 4-days apart

(DOY 71, 1998) **(DOY 75, 1998)**

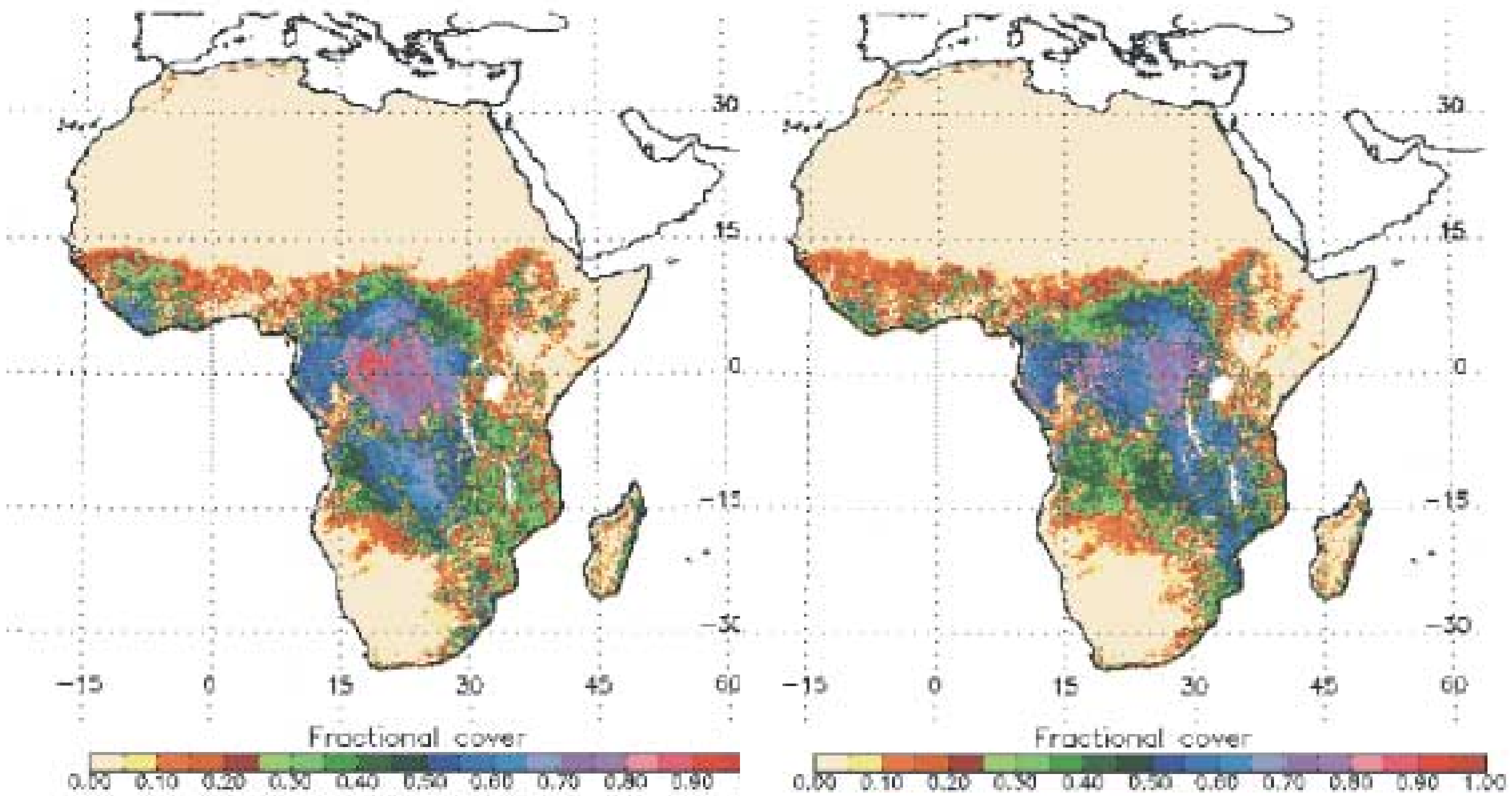

Examining a subset of continent

Extracted box:

- 30 x 30 pixels (240 x 240 km^2)

- Homogeneous land cover type (woodland)

-16 days or two cycle of AVHRR (cover all angular variability of AVHRR; significant sample after cloud screening)

- assess angular variation of LST

(DOY 75, 1998)

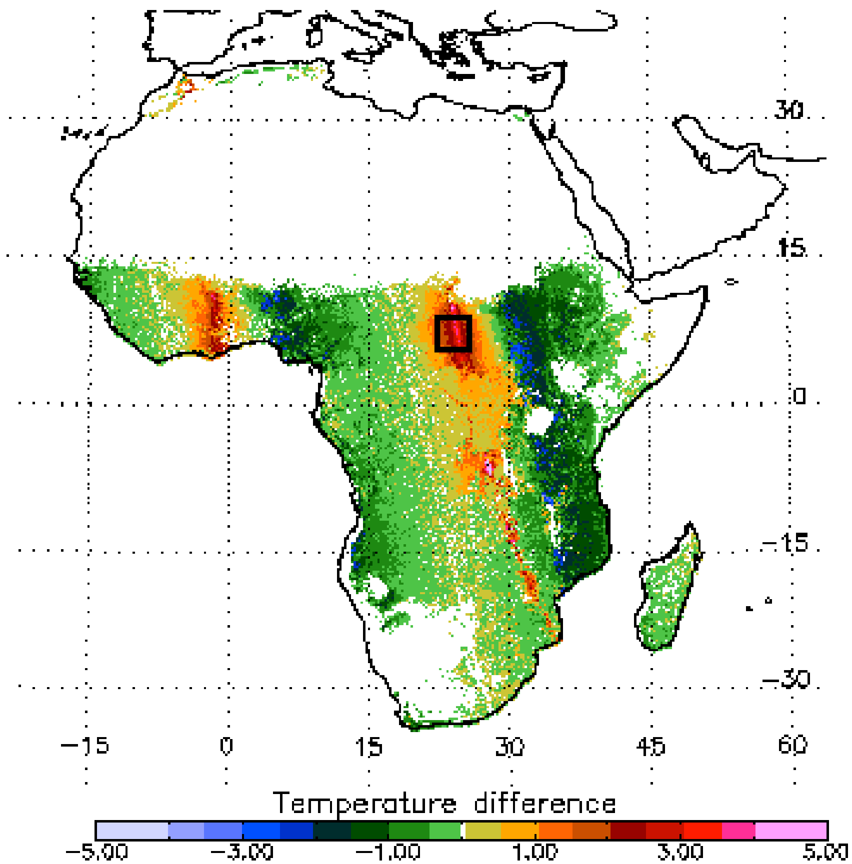

Continental scale: woodland for 1998 vernal equinox

LST vs view zenith angle

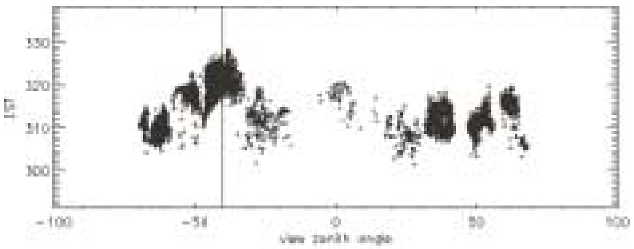

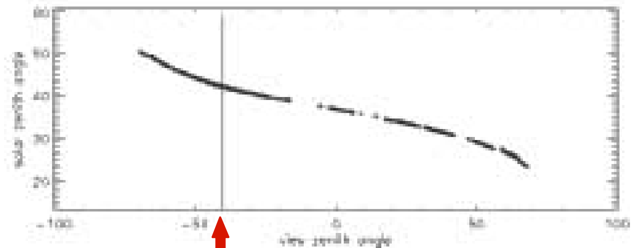

Hot-spot: alignment of illumination and viewing geometries

Sunlit crown

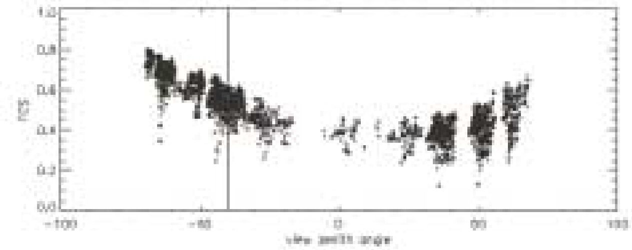

Shaded crown

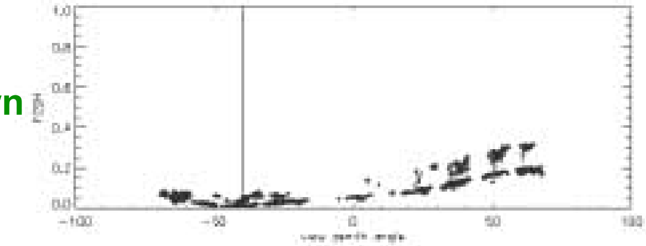

Sunlit background

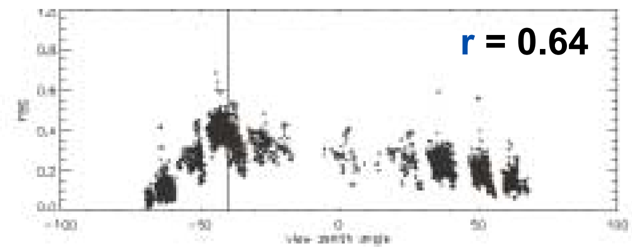

Shaded background

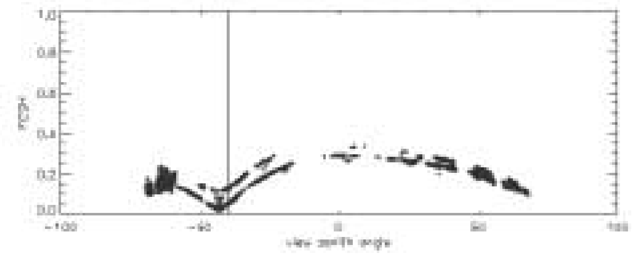

Emissivity fields

- Land cover map
- Continuous fields maps
- FAO soil map Africa
- JPL/JHU spectral library
- AVHRR filter functions

Assume that directional effects on surface temperature observations are dependent on the emissivity angular variation, but are mostly dominated by the structural effects (Snyder, 1998) and an assumption of lambertion end-members is acceptable.

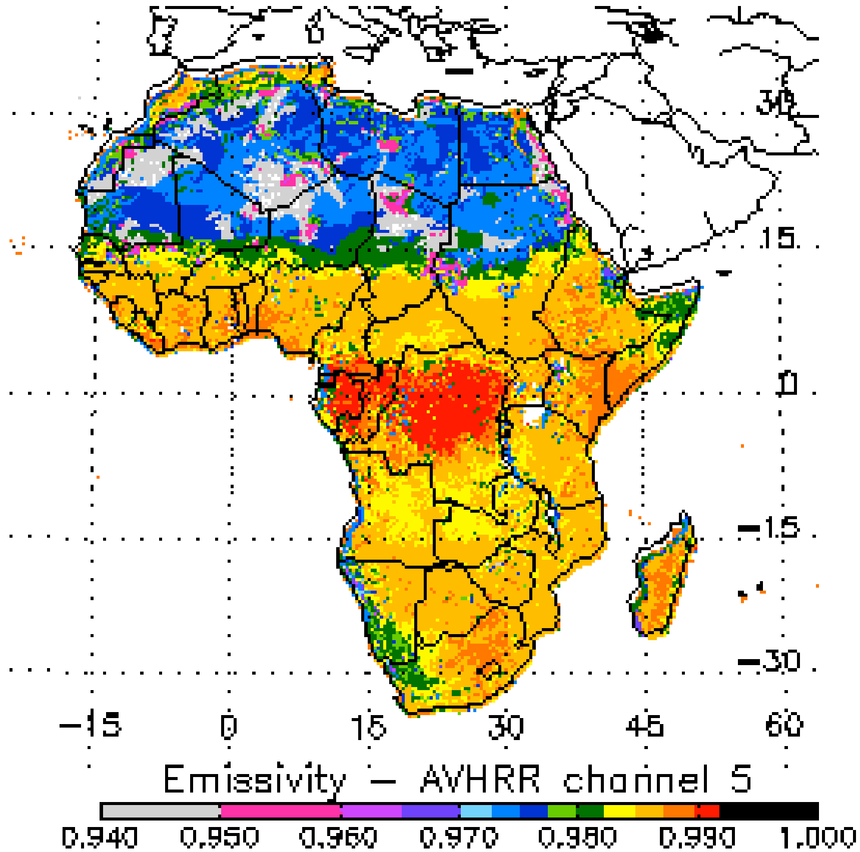

AVHRR channel 5
nadir

Conclusions

- NPP Science Team poised to test EDRs as CDRs
  - Differences in product set (e.g., LAI) and definitions (e.g., Albedo) will be challenging
- MODIS Team expertise and resources have been generously offered
- Pinheiro's Africa Structure and LST project led to new research vein and basis for NPP LST improvements
  - Assimilation into CLM2 Hydrology Model via Postdoc
  - R. Nemani, B. Dickinson, others requesting output
  - Hope to merge GLAS LIDAR with our structure maps soon!

Backup Slides

NPP Provides 27 of 56 NPOESS EDRs

☆	**Atm Vert Moist Profile**
☆	**Atm Vert Temp Profile**
☆	**Imagery**
☆	**Sea Surface Temperature**
☆	Sea Surface Winds
☆	Soil Moisture
	Aerosol Optical Thickness
	Aerosol Particle Size
	Aerosol Refractive Index
	Albedo (Surface)
	Auroral Boundary
	Auroral Energy Deposition
	Auroral Imagery
	Cloud Base Height
	Cloud Cover/Layers
	Cloud Effective Part Size
	Cloud Ice Water Path
	Cloud Liquid Water
	Cloud Optical Thickness
	Cloud Particle Size/Distrib
	Cloud Top Height

Cloud Top Pressure
Cloud Top Temperature
Down LW Radiance (Sfc)
Down SW Radiance (Sfc)
Electric Fields
Electron Density Profile
Energetic Ions
Geomagnetic Field
Ice Surface Temperature
In-situ Plasma Fluctuation
In-situ Plasma Temp
Ionospheric Scintillation
Med Energy Chgd Parts
Land Surface Temp
Net Heat Flux
Net Solar Radiation (TOA)
Neutral Density Profile
Ocean Color/Chlorophyll
Ocean Wave Character
Outgoing LW Rad (TOA)
O^3 – Total Column Profile

Precipitable Water
Precipitation Type/Rate
Pressure (Surface/Profile)
Sea Ice Characterization
Sea SFC Height/TOPO
Snow Cover/Depth
Solar Irradiance
Supra-Therm-Aurora Prop
Surface Type
Active Fires
Surface Wind Stress
Suspended Matter
Total Water Content
Vegetative Index

LEGEND

VIIRS (24)	GPSOS (2)
CMIS (19)	ERBS (5)
CrIS/ATMS (3)	TSIS (1)
OMPS (1)	ALT (3)
SES (13)	APS (4)

☆ - **NPOESS KPPs**

NPP EDRs in black font